

Supporting Information

Enhanced piezoelectric properties and constricted hysteresis behaviour in PZT ceramics induced by Li⁺-Al³⁺ ionic pairs

Y. Feng,^a W. L. Li,^{a,b} D. Xu,^a W. P. Cao,^a Y. Yu,^a and W. D. Fei^{a,*}

^a School of Materials Science and Engineering, Harbin Institute of Technology, Harbin 150001, P.R. China.

^b National Key Laboratory of Science and Technology on Precision Heat Processing of Metals, Harbin Institute of Technology, Harbin 150001, P.R. China.

* Corresponding Author

Email: wdfei@hit.edu.cn

Tel/Fax: +86-451-86413908

The reason why we choose the Li^+ and Al^{3+} is as follows.

For the A-site substitution, there are several requirements for the $\text{A}_1^+-\text{A}_2^{3+}$ ionic pairs. Firstly, the formation of $\text{A}_1^+-\text{A}_2^{3+}$ ionic pairs should keep the local charge neutrality. Because the A-site (Ba^{2+} or Pb^{2+}) valence is +2, equal to the average valence of monovalent and trivalent cation, the local charge neutrality and stoichiometric substitution of monovalent and trivalent cations in A-sites can be maintained. Secondly, the enhanced effect of ionic pairs on piezoelectric properties is caused by local lattice distortion and lower symmetry. Thus, larger the local lattice distortion is, the more piezoelectric enhancement we can achieve. Smaller substitutions can undoubtedly result in larger lattice distortion. The Li^+ is the typical monovalent cation and the valence (+1) is stable in the compounds. For the trivalent cation, the Al^{3+} with smaller ionic radius is regarded as the candidate. In our preliminary studies, the enhanced effect of $\text{Li}^+-\text{Al}^{3+}$ ionic pairs on piezoelectric properties of the BaTiO_3 ceramic has been confirmed.^{1, 2} The aim of this paper is to research the effect of $\text{Li}^+-\text{Al}^{3+}$ ionic pairs on ferroelectric and piezoelectric properties of PZT-based ceramics. According to the existing experimental results, the concept of $\text{A}_1^+-\text{A}_2^{3+}$ ionic pairs is not generalized but specific ($\text{Li}^+-\text{Al}^{3+}$ ionic pairs). Further studies should be done in order to determine whether there are other forms of $\text{A}_1^+-\text{A}_2^{3+}$ ionic pairs existing in the ABO_3 systems (A:+2 and B:+4).

The discussions on the preferential distribution of Li⁺-Al³⁺ ionic pairs are as follows.

It should be noted that, the variation of $I_{(002)}/I_{(200)}$ with dopant content, would not possibly come from the random distribution of Li⁺ and Al³⁺ ions. Assuming that Li⁺ and Al³⁺ ions randomly distribute in all the crystal planes and occupy the A-sites, the trend of the diffracted intensity of (002) peak will be identical to that of (200) peaks, as a consequence of the same structure factor (F) for (002) and (200) diffractions. The $I_{(002)}/I_{(200)}$ with dopant content will be almost unchanged. Thus, there is other reasonable explanation which is consistent with our experimental results. On the basis of defect symmetry principle proposed by Ren *et al.*, Li⁺ and Al³⁺ ions would directly constitute the defect dipole (Li⁺-Al³⁺ ionic pair) in the same cell as many as possible in order to minimize the electrostatic energy and keep local charge neutrality.³⁻⁶ For A-sites replacement, there are two kinds of distributions for Li⁺-Al³⁺ ionic pair: preferential distribution parallel to [001] direction or vertical to [001] direction. Due to the average ionic radius of Li⁺ and Al³⁺ smaller than that of Pb²⁺, the presence of Li⁺-Al³⁺ pairs will induce local lattice distortion of PZT, thus reducing the diffracted intensity of X-ray in the distorted direction. For (002) and (200) planes, the effective structure factors F_{002}^{eff} and F_{200}^{eff} , adjusted by lattice distortion, can be expressed as follows,^{2, 7, 8}

$$F_{200}^{eff} = \bar{F}_{200} \exp\left(-\frac{8\pi^2 \sin^2 \theta}{\lambda^2} \Delta x^2\right) = \bar{F}_{200} \exp(-M_1) \quad (S1)$$

$$F_{020}^{eff} = \bar{F}_{020} \exp\left(-\frac{8\pi^2 \sin^2 \theta}{\lambda^2} \Delta y^2\right) = \bar{F}_{020} \exp(-M_2) \quad (S2)$$

$$F_{002}^{eff} = \bar{F}_{002} \exp\left(-\frac{8\pi^2 \sin^2 \theta}{\lambda^2} \Delta z^2\right) = \bar{F}_{002} \exp(-M_3) \quad (S3)$$

where \bar{F}_{200} , \bar{F}_{020} and \bar{F}_{002} are the average structure factors in the undoped crystals and Δx^2 , Δy^2 and Δz^2 are the mean square displacements in [100], [010], and [001] directions, respectively, which deviate from ideal lattice sites of PZT. Because the

diffracted intensity (I) is proportional to the structure factor's square modulus ($|F|^2$), the following expression can be obtained,

$$I_i \propto \exp(-2M_i) \quad (\text{S4})$$

where the subscript “ i ” corresponds to (200), (020), and (002) plane, respectively.

According to the above expressions, lattice distortion is undoubtedly one of important factors that affect diffracted intensity of X-ray. Considering the results in Figure 1(d), it is believed that both M_1 (equation S1) and M_2 (equation S2) values are much smaller than M_3 (equation S3). In this case, lattice distortion has little impact on the diffracted intensity of (200) plane, but make the diffracted intensity of (002) plane weakened with increasing lattice distortion as shown in Figure 1(d). Based on the above analysis, we may come to a conclusion that Li^+ - Al^{3+} ionic pair tend to arrange parallel to [001] direction. Under the circumstances, the lattice distortion, induced by doped Li^+ and Al^{3+} ions with smaller ionic radius than Pb^{2+} ions, mainly occurs in [001] direction. Therefore, $I_{(002)}$ decreases more quickly than $I_{(200)}$ with dopant content, namely, $I_{(002)}/I_{(200)}$ has a downtrend.

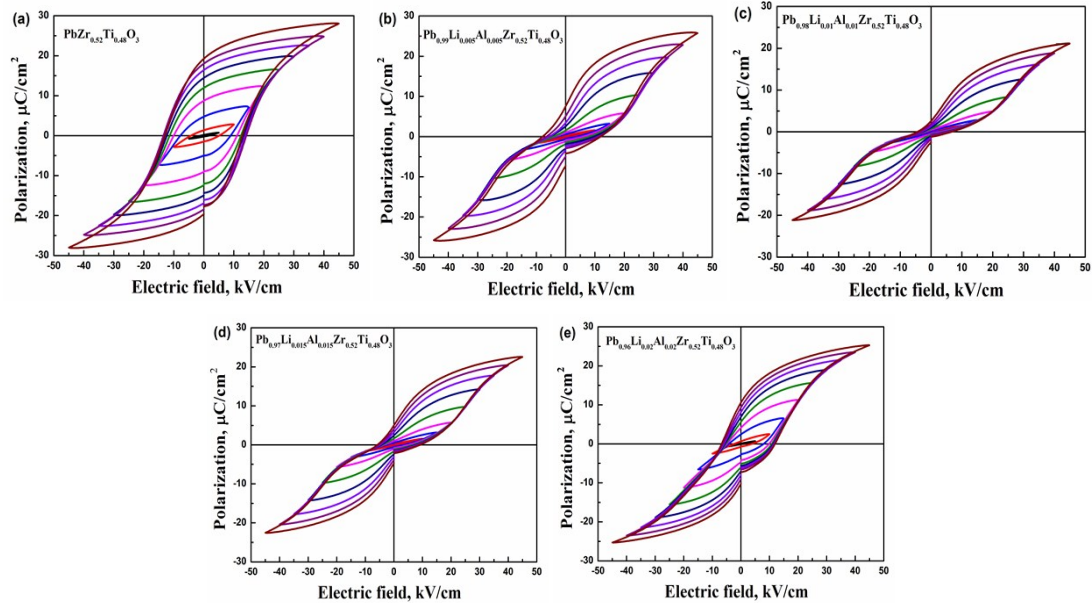


Figure S1 *P-E* loops of the poled PZT ceramic after prolonged storage measured under different electric field: (a) 0 mol.%, (b) 0.5 mol.%, (c) 1 mol.%, (d) 1.5 mol.% and (e) 2 mol.%.

The *P-E* loops of the poled PZT ceramic after prolonged storage measured under different electric field are shown in Figure S1. The *P-E* loops measured under different electric field in the pure PZT ceramic shows a typical ferroelectric behaviour in Figure S1(a). The constricted hysteresis loops are observed in Figures S1(b), (c) and (d), corresponding to the PLA-ZT ceramics doped by 0.5, 1 and 1.5 mol.%, respectively. It is noted that the constricted hysteresis loops in Figures S1(b), (c) and (d) gradually lose the constricted characterization with the applied electric field increasing. This performance meets the character of “electrostatic pinning” and the description of “symmetry conforming principle of point defect” proposed by Arlt and Ren, respectively.^{6, 9} Moreover, the shifts of the hysteresis loops observed in Figures S1(b), (c), (d) and (e) are also a significant manifestation of defect dipole.

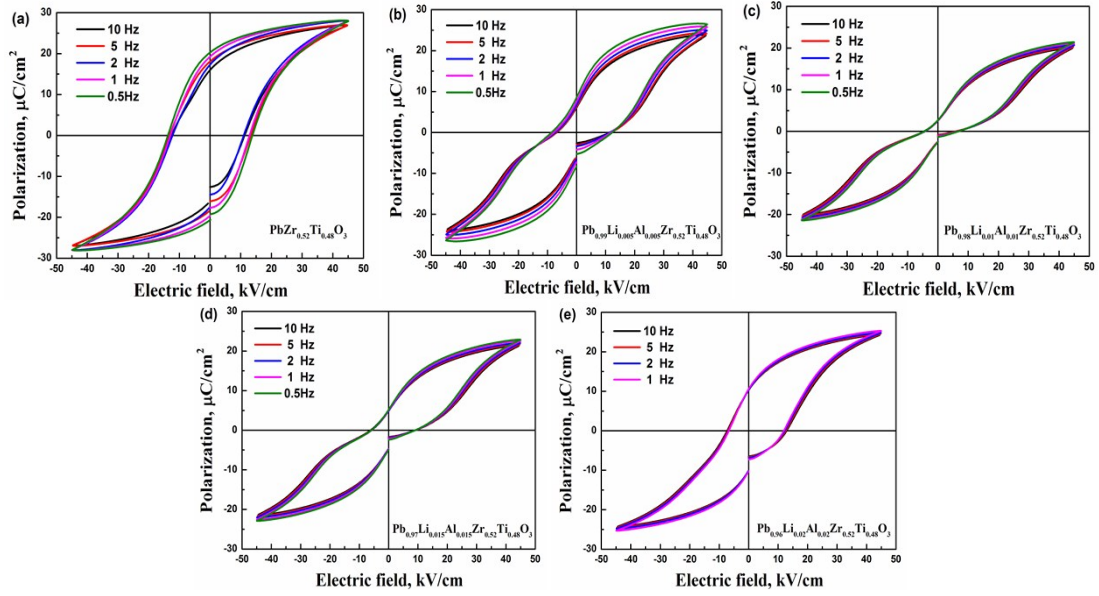


Figure S2 *P-E* loops of the poled PZT ceramic after prolonged storage measured at different frequencies: (a) 0 mol.%, (b) 0.5 mol.%, (c) 1 mol.%, (d) 1.5 mol.% and (e) 2 mol.%.

The *P-E* loops of the poled PZT ceramic after prolonged storage measured at different frequencies are shown in Figure S2. The pure PZT ceramic exhibits well-saturated and normal *P-E* loops at different frequencies (10, 5, 2, 1 and 0.5 Hz). Meanwhile, the constricted hysteresis loops of the doped ceramic in Figures S2(b), (c) and (d) remain almost unchanged with the frequency decreasing to 0.5 Hz. This variation is different from the results in the acceptor doped BaTiO₃ or KNN systems.¹⁰ This phenomenon demonstrates that the electrostatic pinning effect of Li⁺-Al³⁺ defect dipoles on ferroelectric properties of the host materials may be different from that of the cation-oxygen vacancy defect dipole.

References

1. Y. Feng, W. L. Li, D. Xu and W. D. Fei, *Ferroelectrics*, 2015, **489**, 156-163.
2. D. Xu, W. L. Li, L. D. Wang, W. Wang, W. P. Cao and W. D. Fei, *Acta Mater*, 2014, **79**, 84-92.
3. L. X. Zhang and X. Ren, *Phys Rev B*, 2005, **71**, 174108.
4. Z. Y. Feng and X. B. Ren, *Phys Rev B*, 2008, **77**, 134115.
5. M. Unruan, T. Sareein, J. Tangsritrakul, S. Prasertpalichatr, A. Ngamjarurojana, S. Ananta and R. Yimnirun, *J Appl Phys*, 2008, **104**, 124102.
6. X. B. Ren, *Nat Mater*, 2004, **3**, 91-94.
7. Y. M. Wang. X-ray Diffraction of noncrystal and crystal with defects. 1st ed. Beijing: Science Press; 1988 [in Chinese].
8. D. Xu, L. D. Wang, W. L. Li, W. Wang, Y. F. Hou, W. P. Cao, Y. Feng and W. D. Fei, *Phys Chem Chem Phys*, 2014, **16**, 13078-13085.
9. G. Arlt and H. Neumann, *Ferroelectrics*, 1988, **87**, 109-120.
10. D. M. Lin, K. W. Kwok and H. L. W. Chan, *Appl Phys Lett*, 2007, **90**, 232903.